

HI-BRIDGE RESONANT SOFT-SWITCHED BOOST CONVERTER

¹ELANGO VAN.S, ²MARIMUTHU. M, ³VIJYALASKMI

^{1,2,3}Department of Electrical and Electronics Engineering, Saranathan College of Engineering, Triuchirapalli, India.
Email: elangovanselvam@rocketmail.com, Marimuthu-eee@saranathan.ac.in, vijyalakshmi-eee@saranathan.ac.in

Abstract -This paper presents a high step-up DC-DC converter. The proposed converter comprises of a boost converter with an auxiliary switch and resonant circuit. The resonant circuit consists of a resonant inductor, two resonant capacitors, two diodes and an auxiliary switch. These resonant components make partial resonant path for the main and auxiliary switch to perform soft switching under the zero voltage condition using the resonant circuit. The proposed boost converter improves the whole system's efficiency, by reducing the switching losses. The proposed soft switching boost converter has been simulated in PSIM software. The performance of the proposed boost converter is verified through the theoretical analysis and simulation results.

Keywords- Auxiliary resonant circuit, soft-switching boost converter, zero voltage switching (ZVS)

I. INTRODUCTION

There is an increased demand for power electronics having reduced size, weight and cost as well as improved dynamic performance. Passive components (inductors and capacitors) typically dominate the size and weight of a power converter. Increased switching frequency leads to a reduction in the required energy storage and permits use of smaller passive components. Furthermore, higher frequency can substantially improve transient performance and control bandwidth. Sufficiently high frequencies permit the use of air-core magnetics, paving the way towards fully integrated power converters. Thus, many benefits can be realized by operating power converters at greatly increased switching frequencies if loss, efficiency, and control challenges can be addressed.

By introducing resonant auxiliary circuit (Hi-Bridge resonant circuit) to make soft switching. Soft switching techniques such as Zero voltage switching (ZVS), Zero current switching (ZCS) can reduce the switching losses and Electromagnetic interference by putting some stress on the devices. When either current or voltage is zero during the turn ON or turn OFF period, then the product of the voltage and current becomes zero, which leads to zero power loss. Hence the switching loss can be eliminated and the device can operate at high switching frequency. Size and weight of the device is reduced turn-off di/dt in the output rectifier. Several soft-switching converters have been previously proposed to reduce switching loss across the main switch and thus results increasing in system efficiency

The voltage and current stresses on the auxiliary circuit components are high and so are the conduction losses. This paper introduces a soft switching resonant boost converter topology and control method suitable for designs at very high frequency. The topology provides low switch voltage stress, and requires small passive components, allowing for

small size and very fast transient response. Moreover, this design improves the system's efficiency. In this paper, simulation results are presented for a 40W, 30 KHz prototype boost converter using IGBT.

This paper is organized as follows. Section I introduces the research motive. Section II gives a brief description about the modes of operation of the proposed converter. Section III describes about analysis and design procedure. Section IV gives the simulation studies. Section V presents a switching losses and efficiency. Finally, Section VI presents a conclusion.

II. OPERATIONAL PRINCIPLES AND MODES OF THE PROPOSED CONVERTER

A. DEFINITIONS AND ASSUMPTIONS

The circuit scheme of new soft switching boost converter is given in Fig. 1. The proposed converter consists of main switch S1 and the auxiliary switch S2 which enable soft switching through an auxiliary switching block. Auxiliary switching block consists of an auxiliary switch, two resonant capacitors (Cr and Cr2), a resonant inductor (Lr), and two diodes (D1 and D2). The following assumptions are made to simplify the steady state analysis of the circuit given in Fig. 1 during one switching cycle.

1. The input voltage (V_{in}) is constant.
2. The output voltage (V_o) is constant or the output capacitor (C_o) is large enough.
3. All switching devices and passive elements are ideal.
4. The reverse recovery time of all diodes are ignored.

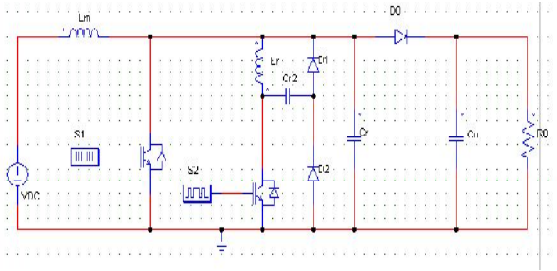


Fig 1. Circuit scheme of the proposed soft switching boost converter.

B. Operation Modes

Nine modes occur in the steady state operation of the proposed converter over one switching cycle. The equivalent circuit schemes of the operation modes are given in Fig. 2. The detailed analysis of the converter is presented as follows.

Mode 1[t0<t<t1:Fig. 2]: At the beginning of this mode all the switches are turned OFF. In this mode, the energy accumulated in the main inductor (L) is transferred to the load through the main diode (D0). The main inductor voltage and current in this mode are represented by (1) and (2). During this time, the resonant inductor current is zero and the resonant capacitor (Cr) has been charged to the output voltage.

$$V_L(t) = V_{in} - V_o \tag{1}$$

$$I_L(t) = (1/L) \int V_L dt \tag{2}$$

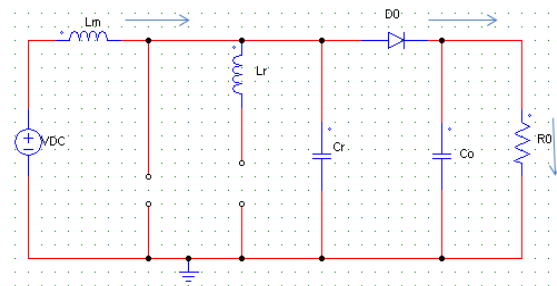


Fig. 2. Mode 1 equivalent circuit.

Mode 2[t1<t<t2:Fig. 3]: In this mode S2 is made to turn ON. After turning ON the auxiliary switch (S2), the resonant inductor current begins to increase linearly from zero. At t2, the resonant inductor current (ILr) is equal to the main inductor current (IL) and mode 2 completes. Thus, the resonant inductor current is expressed by (3).

$$I_{Lr}(t) = (V_o/L_r) (t - t_1) \tag{3}$$

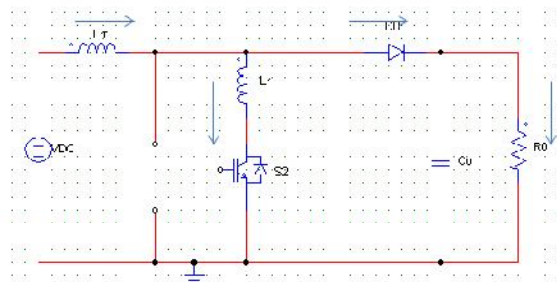


Fig. 3. Mode 2 equivalent circuit.

Mode 3[t2<t<t3:Fig. 4]: This mode begins when the main diode (D0) is turned OFF, immediately after the resonant inductor current and the main inductor current have been equalized. Then resonant capacitor Cr and resonant inductor Lr starts their resonance and Cr is discharged through resonant path Cr and Lr. After finishing resonance, the resonant capacitor voltage is equal to zero and mode 3 completes at t3. During this mode, the resonant impedance and angular frequency are given by Zr and ωr.

$$t_1 = I_L / (V_o/L_r) \tag{4}$$

$$I_{Lr}(t) = I_{min}(t) + (V_o/Z_r) \sin \omega_r (t - t_2) \tag{5}$$

$$V_{Cr}(t) = V_o \cos \omega_r (t - t_2) \tag{6}$$

$$Z_r = \sqrt{L_r/C_r}; \omega_r = 1/\sqrt{L_r C_r} \tag{7}$$

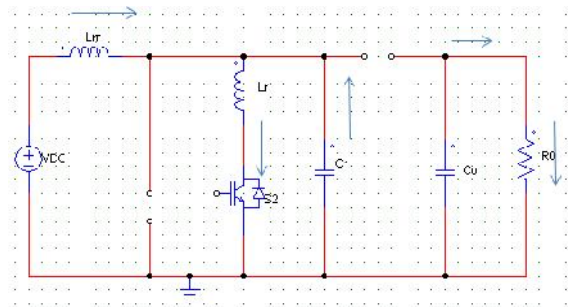


Fig. 4. Mode 3 equivalent circuit.

Mode 4[t3<t<t4:Fig. 5]: As soon as the resonant capacitor (Cr) voltage has reached zero, the body diode of the main switch S1 turns ON naturally. In this case, the main switch voltage is equal to zero and the turn ON signal is given to the main switch under the zero voltage condition.

$$I_{Lr}(t) = (V_o/L_r) (t - t_1) \tag{8}$$

$$V_{Cr}(t) = 0, V_{Cr2}(t) = 0 \tag{9}$$

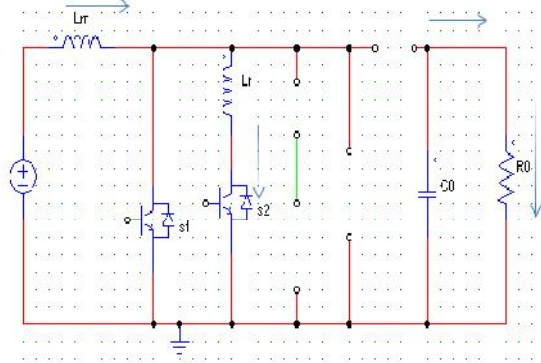


Fig. 5. Mode 4 equivalent circuit.

Mode 5[t4<t<t5:Fig. 6]: This mode begins when the auxiliary switch is turned OFF under zero voltage condition. In this case, inductor Lr and the resonant capacitor Cr2 starts the resonance. Mode 5 ends when Cr2 has been fully charged by resonance. The resonant impedance and angular frequency are given by Za and ωa

$$I_{Lr}(t) = I_{Lr}(t_3) \cos \omega_a (t - t_4) \tag{10}$$

$$\omega_a = 1/\sqrt{L_r C_{r2}}; Z_a = \sqrt{L_r/C_{r2}} \tag{11}$$

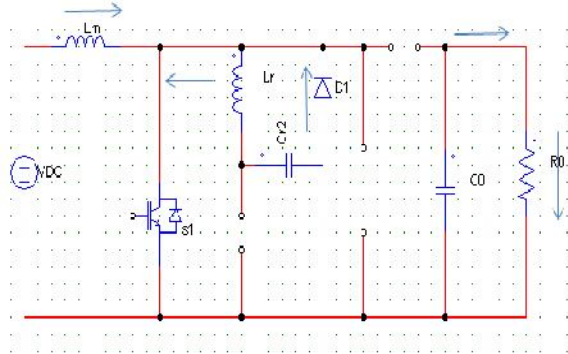


Fig. 6. Mode 5 equivalent circuit.

Mode 6 [t5 < t < t6: Fig. 7]: In this mode, current flow through the resonant inductor Lr reverses and hence a reverse resonance of Lr and Cr2 occurs through the main switch and D2. When Cr2 voltage has reached zero by resonance, the resonance of Lr and Cr2 is complete and thus mode 6 ends.

$$V_{cr2}(t) = Z_{a1} I_{Lr}(t_3) \sin \omega_a (t - t_5) \quad (12)$$

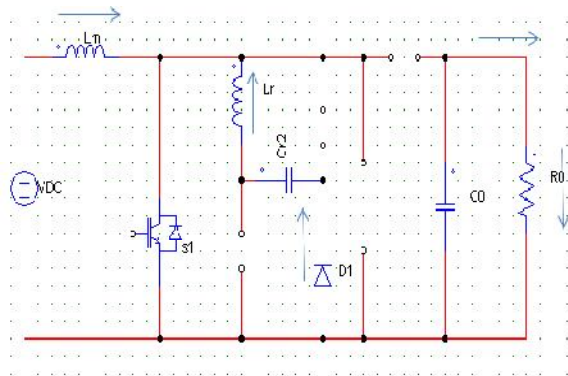


Fig. 7. Mode 6 equivalent circuit.

Mode 7 [t6 < t < t7: Fig. 8]: This mode starts when the body diode of the auxiliary switch is turned ON after the Cr2 voltage has reached zero. When the main switch is turned OFF by PWM algorithm, this mode is completed.

$$I_L(t) = I_{min} + (V_{in}/L)(t - t_3) \quad (13)$$

$$I_{Lr}(t_7) = - I_{Lr}(t_3) \quad (14)$$

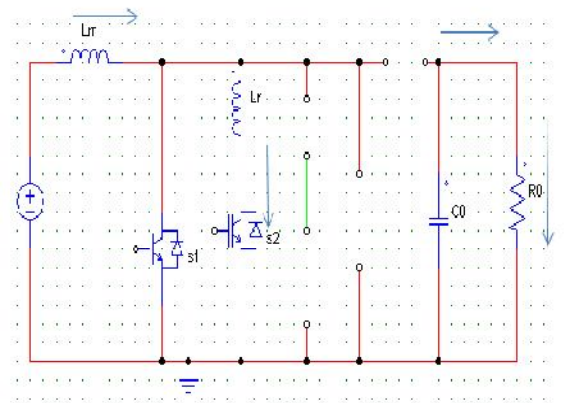


Fig. 8. Mode 7 equivalent circuit.

Mode 8 [t7 < t < t8: Fig. 9]: When the main switch is turned off under the zero voltage condition, mode 8 starts. When the resonant capacitor (Cr) voltage is equal to the output voltage, this mode is completed.

$$I_{Lr}(t) = I_{Lr}(t_7) - (I_{Lr}(t_7) + (I_{Lr}(t_3))) \cos \omega r t \quad (15)$$

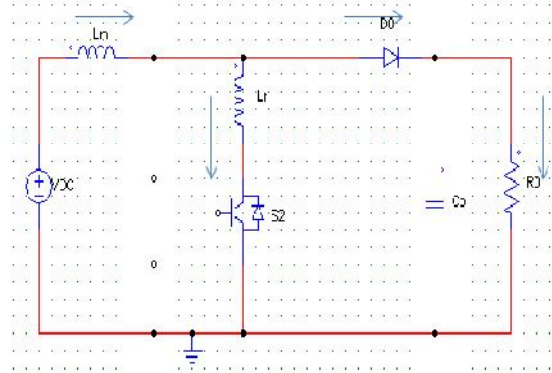


Fig. 9. Mode 8 equivalent circuit.

Mode 9 [t8 < t < t9: Fig. 10]: This mode begins when the main diode D0 turns ON under the zero voltage condition and the resonant inductor current decreases linearly towards zero. After the current has reached zero, mode 9 completes and the next switching cycle starts.

$$I_L(t) = I_L(t) - (V_o - V_{in})/L * t \quad (16)$$

$$I_{Lr}(t) = - I_{Lr}(t_3) + (V_o/Lr)t \quad (17)$$

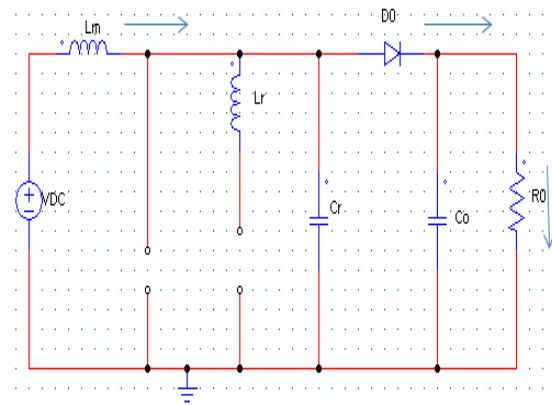


Fig. 10. Mode 9 Equivalent circuit.

III. ANALYSIS AND DESIGN PROCEDURE

This paper discusses the analysis and design procedure of the soft switching boost converter. In steady state operation

1. When both S1 and S2 is OFF.
2. When S1 is OFF and S2 is ON.
3. When S1 is ON and S2 is OFF.

Design procedure of Boost Converter:
 Vin = 12V, Vo=40V, Ro= 10V Io = 4A
 Duty cycle: D= 1-(Vin/Vo) = 0.7

Where $T = 33.33\mu s$ $T_{on} = 23.33\mu s$, $T_{off} = 10\mu s$

Where $\Delta I = 1.25$ Amps $L = (V_{in} * D) / (\Delta I * F_s) = 560\mu H$

Where $\Delta V_c = 0.7V$

$C = (I_o * D) / (\Delta V_c * F_s) = 100\mu F$

Applying volt-second balance for main inductor (L):
 $V_L(t) = V_{in}(D_{aux} - (T_r/T)) + V_{in}(D_{aux} + (T_r/T)) + (V_{in} - V_o)(1 - D_{aux} - D_{main})$
 Where T_r is the resonant time between the resonant inductor and resonant capacitor. Hence, the voltage conversion ratio is given by the following equation

$$V_o/V_{in} = 1 / (1 - (D_{aux} + D_{main})) \quad (16)$$

If the charging voltage of the resonant capacitor (C_{r2}) is higher, the voltage stress of the switch is higher. Consequently, this voltage must be lower than the output voltage given by (13). The resonant time for mode 5 as 0.2 of DTs. Hence the angular frequency and resonance impedance is given by

$$\pi \sqrt{L_r C_{r2}} \leq 0.1 T_s$$

$$\omega a = 942477.8 \quad Z_a \leq 71.8$$

$$L_r = (Z_a / \omega a), \quad C_{r2} \geq (1 / Z_a^2 * \omega a)$$

$$L_r = 35\mu H, \quad C_{r2} = 30\mu F$$

Using the design values various simulation results are performed in next section.

IV. SIMULATION STUDIES

Simulation studies of the proposed DC-DC converter are undertaken using PSIM. The simulation was performed for a switching frequency of 30 KHz.

Table 1

Input Voltage(V_{in})	12V
Output Voltage(V_o)	40V
Switching Frequency(F_s)	30KHZ
Resonant Inductor(L_r)	560 μH
Main Inductor(L)	100 μH
Resonant Capacitor(C_r)	3.3nF
Resonant Capacitor(C_{r2})	30nF

A. Open – loop conventional Boost Converter
 Fig.11. shows the simulated circuit diagram for the open loop voltage control of the conventional boost converter.

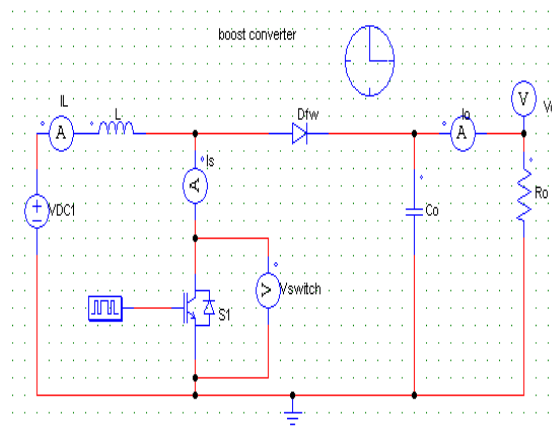


Fig.11. shows the simulated scheme of open loop voltage control of the conventional boost converter.

Switch mode power supply has been smaller and lighter because the switching frequency is higher. But as the switching frequency is higher, the periodic loss increases at turn on and turn off. As a result, this loss increases the losses of whole system. This can shows in fig 14

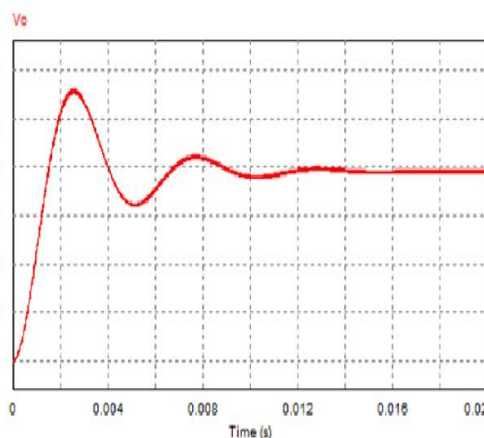


Fig. 12. Conventional boost converter output voltage

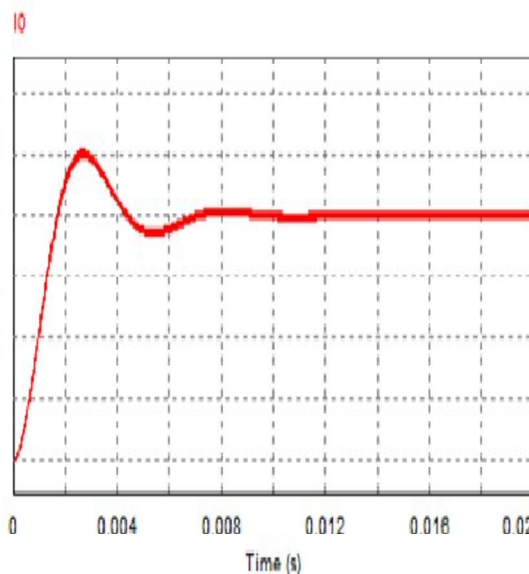


Fig. 13. Conventional boost converter output current

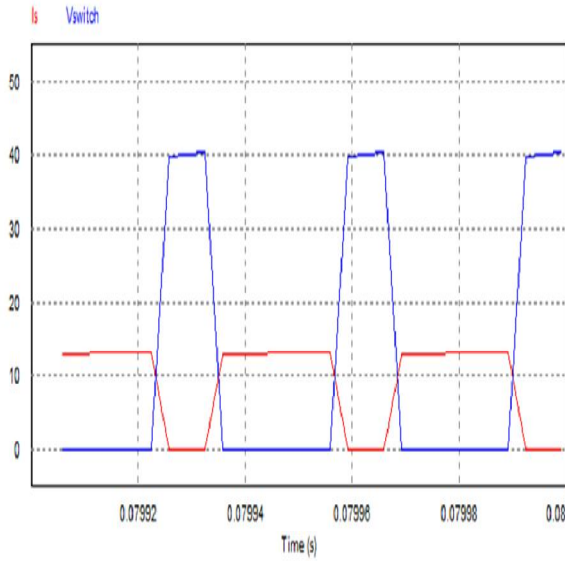


Fig. 14. Switching voltage and current waveform of conventional boost conventional.

Conventional Boost Converter circuits have more losses across the switch when the switch turn ON and turn OFF. This results in reduction in system efficiency.

B. Open – loop Proposed Boost Converter

Fig.15. shows the simulated circuit diagram for the open loop voltage control of the proposed converter. Before the main switch is turned ON, the body diode is turned ON; hence the main switch enables zero voltage switching.

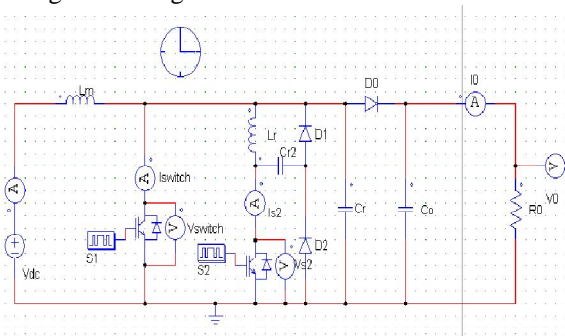


Fig 15. Simulated circuit diagram for open loop voltage control of Proposed Boost Converter

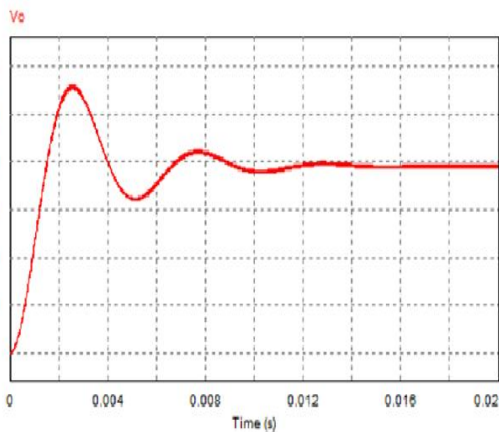


Fig. 16. Proposed converter output voltage

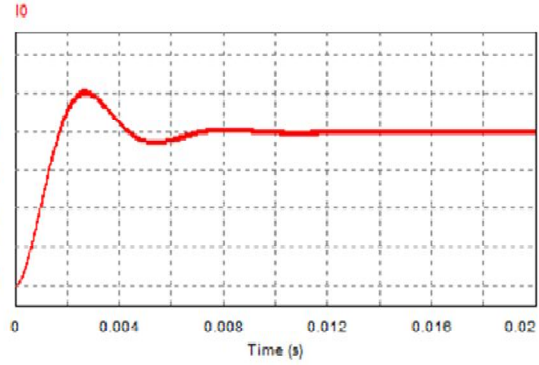


Fig.17. Proposed converter output current.

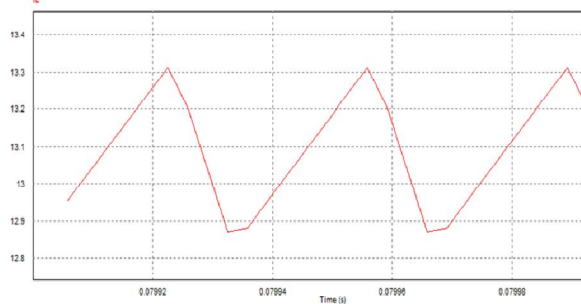


Fig. 18. Main inductor current of proposed converter.

Fig. 19. Shows the main switch is turned ON, the body diode is turned ON, and hence the main switch enables zero voltage switching. Voltage and Current Waveform of main switch

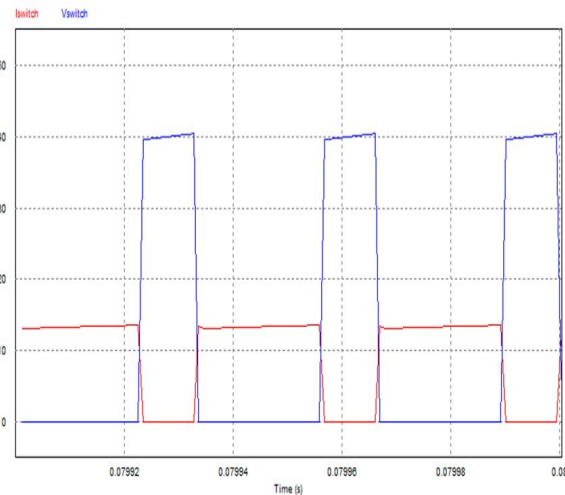


Fig. 19. Main switching voltage and current showing ZVS.

Conventional Boost Converter circuits have more losses across the switch when the switch turn ON and turn OFF. This results in reduction in system efficiency. By introducing proposed topology the generations of switching losses are avoided by forcing voltage (ZVS) to zero during switching. The efficiency is improved due to reduction in switching losses.

C. Closed – loop Proposed Boost Converter

Fig. 4 shows the simulated circuit diagram for the closed loop voltage control voltage of the proposed DC-DC converter. At an input voltage of 12V-35V, the output voltage can be adjusted to 40V by

incorporating the closed loop control. The output is sensed using a voltage sensor and is fed to the PI controller through an error amplifier. The gain of the PI controller is 0.555.

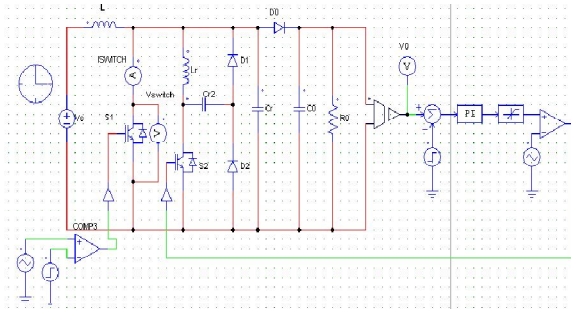


Fig . 20. Closed loop voltage control of proposed boost converter.

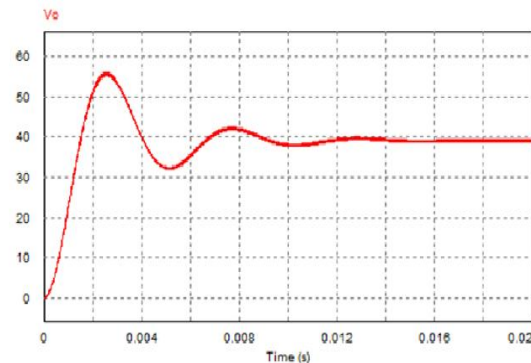


Fig. 21. Closed loop proposed boost converter output voltage

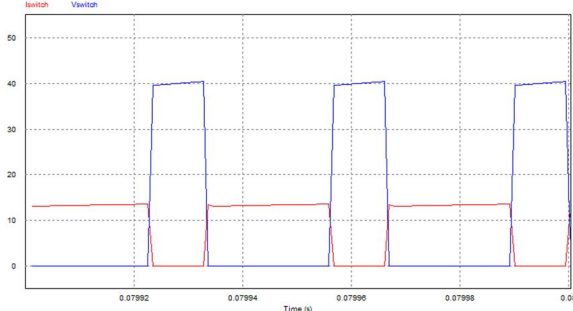


Fig. 22. Closed loop proposed boost converter switching voltage and current

V. SWITCHING LOSSES AND EFFICIENCY

Power loss across the switch can be calculated from the fig.

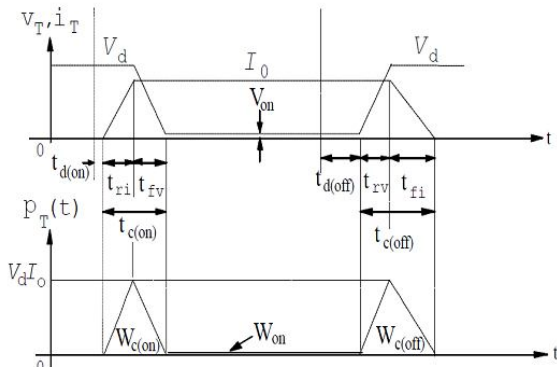


Fig . 22. Waveform of switching characteristics.

Figs. 22. Show the waveform of switching losses across the switch during turn on and turn off. The average switching power loss (Ps) across the switch.

$$P_{Loss} = V_o * I_o * F_s * (T_c(on) + T_c(off)) / 2 \quad (17)$$

Where, $t_c(on)$ - turn-on crossover interval
 $t_c(off)$ - Turn-off crossover interval

By using above waveform calculate the power losses across the switch in both conventional and proposed boost converter.

EFFICIENCY COMPARISON OF THE PROPOSED BOOST CONVERTER WITH THE CONVENTIONAL BOOST CONVERTER.

A. Conventional boost conversion

The average switching power loss P_s across the switch S1 by using (17)

$$P_{Loss} = 40 * 13 * [2.5 * 10^{-6}] * 30000 = 39W$$

B. Proposed Boost Converter

The average switching power loss P_s across the main switch S1 after applying soft-switching by using (17)

$$P_{Loss} = 40 * 13 * [1.0 * 10^{-6}] * 30000 = 16W$$

EFFICIENCY

A. Conventional boost converter

$$\begin{aligned} \text{Efficiency} &= P_{out} / P_{in} \\ &= ((40 * 4) / ((40 * 4) + 39)) \\ &= 81\% \end{aligned}$$

B. Proposed boost converter

$$\begin{aligned} \text{Efficiency} &= P_{out} / P_{in} \\ &= (((40 * 4) / ((40 * 4) + 16)) \\ &= 92\% \end{aligned}$$

Using soft-switching techniques losses across the switch reduce and Efficiency of the system increased. The graph is plotted between efficiency and input voltage (V_{in}) for different values. It is found that the efficiency of the proposed boost converter is increased due to soft switching compared to the conventional boost converter are showing in fig. 23.

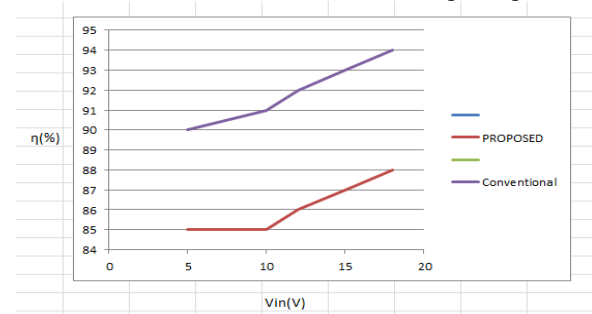


Fig. 23. Efficiency comparison waveform.

CONCLUSION

This paper has proposed a high efficiency soft switching boost converter which uses a resonant circuit and an auxiliary switch. Both the main and the auxiliary switch perform soft switching under the zero voltage condition. Compared with the conventional boost converter, the proposed converter has higher efficiency and more voltage boost effect. A simulation result of the proposed converter for open loop voltage controls is provided for a switching frequency of 30 KHz. The results are found to agree with the theoretical analysis presented in this paper.

REFERENCES

- [1] B.R. Lin, B.R. Hou, "Analysis of a zero voltage switching DC/DC converter without output inductor," *IET Trans. Power Electron.*, vol. 5, no. 6, 790 – 800, July 2012
- [2] G. Hua, E. X. Yang, Y. Jiang, and F. C. Y. Lee, "Zero-Voltage and Zero-Current-Switching PWM Combined Three-Level DC/DC Converter," *IEEE Trans. Power Electron.*, vol. 57, no. 5, pp. 1644– 1645, May 2010.
- [3] H. Bodur and A. F. Bakan, "A new ZVT-ZCT-PWM DC-DC converter," *IEEE Trans. Power Electron.*, vol. 19, no. 3, pp. 676–684, May 2004.
- [4] H. Bodur and S. Cetin, G. Yanik, "A Zero-Voltage-Switching Bidirectional DC–DC Converter With State Analysis and Soft-Switching-Oriented Design Consideration," *IEEE Trans. Industrial Electron.*, vol. 56, no. 6, pp. 2174–2184, June 2002.
- [5] S. S. Saha, B. Majumdar, T. Halder, and S. K. Biswas, "Analysis and Implementation of a ZVS/ZCS DC– DC Switching Converter with Voltage Step-Up," *IEEE Trans.*, vol. 58, no. 7, pp. 2962–2971, Jan. 2004.
- [6] N. Jain, P. K. Jain, and G. Joos, "A zero voltage transition boost converter employing a soft switching auxiliary circuit with reduced conduction losses," *IEEE Trans. Power Electron.*, vol. 19, no. 1, pp. 130–139, Jan. 2004.
- [7] S.H. Park, S.R. Park, J.S. Yu, Y.C. Jung and C.Y. Won, "Analysis and design of a soft switching boost converter with an HI-bridge auxiliary resonant circuit," *IEEE Trans. on Power Electronics*, vol. 25, no. 8, pp. 2142-2149, August 2010.
- [8] Tsai-Fu Wu, Yong-Dong Chang, Chih-Hao Chang, Jeng-Gung Yang, "Soft-Switching Boost Converter with a flyback Snubber for High Power Applications," *IEEE Trans. on Power Electronics*, vol. 27, no. 3, pp. 1108-1119, Mar. 2010.
- [9] H. Mao, O. A. Rahman, and I. Batarseh, "Zero-voltage-switching DC-DC converters with synchronous rectifiers," *IEEE Trans. Power Electron.*, vol. 23, no. 1, pp. 369–378, Jan. 2008.

★★★